Published in final edited form as:
Biochim Biophys Acta. 2010 June ; 1804(6): 1376–1384. doi:10.1016/j.bbapap.2010.02.014.

Differential Modulation of the Active Site Environment of Human Carbonic Anhydrase XII by Cationic Quantum Dots and Polylysine

Sumathra Manokaran[1], **Xing Zhang**[2], **Wei Chen**[2], and **D. K. Srivastava**[1,*]

[1]Department of Chemistry, Biochemistry and Molecular Biology, North Dakota State University, Fargo, ND 58105

[2]Department of Physics, University of Texas at Arlington, TX 76010

SUMMARY

Due to prevalence of negative charges on the protein surface, opposite to the active site pocket of human carbonic anhydrase XII (hCA XII), both positively charged CdTe-quantum dots (Qds^+) and polylysine electrostatically interact with the enzyme, and such interaction does not influence the catalytic activity of the enzyme. However, both these cationic macromolecules differently modulate the active site environment of the enzyme. The steady-state kinetic data revealed that whereas polylysine exhibited no influence on dansylamide (DNSA) dependent inhibition of the enzyme, Qds^+ overcame such an inhibitory effect, leading to almost 70% restoration of the catalytic activity of the enzyme. We provide evidence that DNSA remains bound to the enzyme upon interaction with both polylysine and Qds^+. Arguments are presented that the above differential feature of polylysine and Qds^+ on hCA XII is encoded in the "rigidity" versus "flexibility" of these cationic macromolecules.

Keywords

Carbonic anhydrase XII; Quantum dots; dansylamide; polylysine

INTRODUCTION

Due to their potential diagnostics and therapeutic applications, nanoparticles have gained significant interest in recent years [1–3]. Among nanoparticles, semiconductor quantum dots offer added advantage due to their broad absorption and narrow emission bands, size tunable fluorescence emission spectra, longer fluorescence lifetimes, and resistance to photo bleaching [4–10]. Quantum dots (Qds) are considered to be an important diagnostic tool as they have the ability to enter all parts of the body including the brain via receptor mediated endocytosis [11]. However, in vivo applications of Qds are limited due to their inherent toxic effects [12–16]. They are, on the other hand, useful for in vitro applications such as

*To Whom Correspondence should be addressed: D. K. Srivastava, Department of Chemistry, Biochemistry and Molecular Biology, North Dakota State University, Fargo, ND 58102; Phone: (701) 231-7831; Fax: (701) 231-8324; dk.srivastava@ndsu.edu.

cell and tissue labeling, detection of specific single macromolecules, immuno staining of proteins etc. [1–4, 11, 17–19].

It has been recognized that as soon as the Qds enter into the blood stream, they are immediately coated with different types of proteins, and depending on the surface properties of the Qds, the overall coating process is manifested by a combination of van der waal's, electrostatic and hydrophobic interactions [20–26]. The adsorption of proteins to Qds surface leads to the changes in the protein conformation and/or changes in the surface of the nanoparticles [27–33]. For example, the interaction of CdS-quantum dots with human hemoglobin results in a significant alteration of its secondary and tertiary structures. This in turn leads to quenching of the intrinsic fluorescence of the protein [27]. In this paradigm, it has been noted that certain nanoparticles induced conformational changes in proteins are isozyme selective [28]. For example, recent NMR data reveals that the silica nanoparticles exhibit completely different impacts on the structure of human carbonic anhydrase I (hCA I) and human carbonic anhydrase II (hCA II). Whereas hCA II interacts strongly with silica nanoparticles leading to an ensemble of molten globule like bound protein states, hCA I interacts (with similar nanoparticles) albeit weakly and leads to a small perturbation in the protein structure on a longer time scale. It is believed that surface curvature of nanoparticles in conjunction with their complementary interactions with cognate proteins induce different types of conformational changes [28].

We have been interested in developing isozyme selective inhibitors as well as diagnostic tools against various pathogenic enzymes including carbonic anhydrases [43, 49]. While working with human carbonic anhydrases, we noted that the surface of human carbonic anhydrase XII (hCA XII; the enzyme implicated in promoting hypoxic tumors) harbors patches of positive and negative charges in the vicinity and opposite side of the enzyme's active site pocket, respectively [34,40]. Such a distinct charge distribution on the surface of hCA XII, prompted us to investigate the role of plausible electrostatic interaction of positively charged macromolecules (on the surface opposite to the active site pocket of hCA XII) in modulating the enzyme's microenvironment. These studies reveal that Qds^+ (but not similarly charged polylysine) alters the microenvironment of the enzyme's active site (via the long range interaction) such that it exhibits full catalytic activity even in the presence of the enzyme bound inhibitor DNSA.

EXPERIMENTAL PROCEDURES

MATERIALS

Tryptone, yeast extract were purchased from Becton Dickinson, Sparks, MD. Polylysine, Phenylmethylsulfonyl fluoride (PMSF), p-aminomethyl benzenesulfonamide (pAMBS) – agarose were obtained from Sigma. DNSA was purchased from Avocado Research Chemicals, Heysham, Lancashire, U.K. Acetonitrile was from Aldrich Chemical Co., Milwaukee, WI. Chloramphenicol, ampicillin, IPTG, Zinc Sulfate were from Life Science Resources, Milwaukee, WI. BL21 expression cells were from Stratagene, La Jolla, CA. Sodium chloride, Tris, EDTA, and Potassium sulfate were purchased from VWR, Westchester, PA. The plasmid encoding the catalytic domain region of the human carbonic anhydrase XII gene was a kind gift from Dr. William Sly of St. Louis University School of Medicine, St. Louis, MO.

METHODS

Preparation of cationic quantum dots—The synthesis of cationic quantum dots (Qds^+) was described in our recent publications [10,34]. The size of the Qds^+ obtained was determined to be approximately 4.5 nm [34].

Determination of concentrations of cationic quantum dots and polylysine—We determined the concentrations of Qds^+ by titrating it by increasing concentrations of hCA XII while monitoring the quenching of the tryptophan fluorescence of the enzyme. Since the binding affinity of hCAXII for Qds^+ was in the nM range, the beginning of the titration curve showed a nearly linear dependence on the enzyme concentration (see Figure 1B) from which the stoichiometry of the enzyme-Qds^+ complex could be easily ascertained by fitting the binding isotherm according to Qin and Srivastava [39]. Since the concentration of hCA XII has been known, the concentration of Qds^+ was calculated from the derived stoichiometry of the resultant complex.

The concentration of polylysine was determined by taking the average molecular weight of the macromolecule as being equal to 24,000 Daltons as per the manufacturer's specification. In all experiments reported herein, we have taken the concentration of entire (i.e., polymeric form) polylysine moiety rather than its monomeric lysine residue.

Expression and purification of hCA XII—The catalytic domain of hCA XII from the original plasmid (pBShCA XII) was amplified by the hot start PCR method, and was cloned in pET20b (+) plasmid expression vector as described previously [34]. The idea was to produce the catalytically active form of hCA XII similar to that utilized for determining the crystal structure of the enzyme [40]. However, due to cloning strategy, our construct contains Met (instead of Ala present in the protein used for the crystallographic studies) at the N-terminus of the protein, and it is devoid of Ser-Gln dipeptide at the C-terminal end. Other than these, our expressed protein is identical to that utilized for determining the X-ray crystallographic structure of hCA XII [40].

The cloned plasmid containing the coding sequence of the catalytic domain of hCA XII was transformed into the *Escherichia coli* BL21-CodonPlus® DE3 (RIL) cells by following the standard molecular biology protocol [35]. The transformed cells were grown at 37º C in LB medium, containing 100 μg/mL of ampicillin, 50 μg/mL of chloramphenicol, and 100 μM of $ZnSO_4$ until A_{600} was 0.8. The temperature was then reduced to 18º C until the absorbance reached 1.0 and was induced using 0.5 mM IPTG and 200 μM $ZnSO_4$. After induction, the cells were allowed to grow at 18 ºC for 12 – 16 hours with constant shaking in an orbital shaker at 300 rpm. The cells were then centrifuged at 5000 rpm for 15 min. The cell pellet obtained after centrifugation was suspended in a buffer containing 20 mM Tris-SO_4 containing 0.5 mM EDTA and 0.25 % Triton X 100, pH 8.0. A total concentration of 1 mM PMSF dissolved in isopropanol was also added prior to sonication. The cells were then placed in an ice-cold bath and sonicated in Branson bath sonifier for 10 min using 40 % duty cycle. After sonication, the suspension was centrifuged at 15,000 rpm for 30 min and the supernatant was used for further purification.

For purification of recombinant hCA XII from supernatant, p-AMBS-agarose was used as the column resin. The column was initially equilibrated with a buffer containing 20 mM Tris-SO_4, pH 8.0. The supernatant was mixed with the gel slurry and stirred for 2 hours and was loaded on a 2 x 12 cm column. The load flow through of the column was discarded. The column was then washed with wash buffer containing 0.1 M Tris-SO_4, 0.2 M K_2SO_4 and 0.5 mM EDTA, pH 9.0, followed by washing with the buffer containing 0.1 M Tris-SO_4 and 0.2 M K_2SO_4, pH 7.0. The elution of the enzyme from the column was carried out using an elution buffer containing 0.1 M Tris-SO_4, 0.4 M KSCN and 0.5 mM EDTA, pH 6.8. All the fractions having absorbance greater than 0.5 were pooled, and were concentrated using a PM-10 ultra filtration membrane and dialyzed against 25 mM HEPES buffer pH 7.5. The protein concentration was determined via the Bradford method [37] using BSA as a standard protein. The purity of hCA XII was determined by SDS-PAGE [38]. The molecular weights of the native and individual subunits were determined by the gel filtration and SDS-PAGE

techniques, respectively. Whereas the molecular weight of the native hCA XII was found to be 60, its subunit molecular weight was found to be 30 kD. Hence, the purified hCA XII is a homodimer as reported by Whittington et. al. [40].

Measurement of the enzyme activity—The catalytic activity of hCA XII was measured by the pH drop method of Wilbur and Anderson [36]. In this method, the time dependent change in pH of a weekly buffered solution (20 mM Tris-HCl, pH 8.3), due to the enzyme catalyzed hydration of CO_2 to generate carbonic acid, is measured at low temperature by the aid of a pH meter. The carbonated solution was prepared by bubbling CO_2 to ice cold Millipore water for about 30 min., and it was kept in the ice bath. For the blank reaction, 4.0 mL of the above carbonated solution was mixed with 6.0 mL of ice cold 20 mM Tris-HCl buffer, pH 8.3, with constant stirring, and the time required (T_0) for the drop in pH from 8.3 to 6.3 was recorded by a pH meter. The above experiment was repeated in the presence of hCA XII in the absence and presence of different ligands, and the time required (T) for the drop in pH from 8.3 to 6.3 was recorded. Given the magnitudes of T_0 and T, the activity of hCA XII was calculated by the relationship: T_0-T)/T. Each activity measurement was performed in duplicate, and the resultant values were averaged. Since the enzyme activity thus calculated is in arbitrary unit, it is represented as the percent of the control activity (100%) in the absence of any ligand.

Spectrofluorometric studies—All the steady-state spectrofluorometric studies involving Qds^+ were performed on a Perkin Elmer LS 50B spectrofluorometer, equipped with a magnetic stirrer and thermostated water bath. Unless otherwise mentioned, all the experiments involving Qds^+ were performed utilizing 10 mM Tris, pH 8.0 as the Qds^+ were found to be stable in this buffer. For experiments involving DNSA, 10% acetonitrile in addition to the above buffer was used. A stock of 1 mM DNSA was prepared in 10 mM HCl and was diluted into 10 mM Tris, pH 8.0, containing 10 % acetonitrile. The stock solution of polylysine was prepared in 25 mM HEPES buffer, pH 7.5. The emission spectrum of the enzyme was taken by fixing the excitation wavelength at 295 nm. Unless mentioned otherwise, the excitation and emission slits were kept at 5 mm each and the PMT voltage was set at 800.

The binding affinity of Qds^+ to hCA XII was determined by titrating a fixed concentration of Qds^+ with increasing concentrations of hCA XII in 10 mM Tris-HCl buffer, pH 8.0. The excitation and emission wavelengths were set at 295 nm and 336 nm, respectively. A fixed concentration of Qds^+ was titrated with known concentrations of hCA XII. A blank titration of protein into buffer was subsequently performed in order to subtract the signal contributed by blank from that of the sample. The difference in the protein emission intensity at 336 nm was plotted as a function of the protein concentration and the dissociation constant of the hCA XII- Qds^+ complex was determined as described by Qin and Srivastava [39].

The binding isotherm for the interaction of polylysine with hCA XII in the presence of DNSA was determined by titrating a fixed concentration of hCA XII (1 μM) and saturating concentration of DNSA (5 μM) by increasing concentrations of polylysine in 25 mM HEPES buffer , pH 7.5, containing 10 % acetonitrile. The excitation wavelength was set at 330 nm and the decrease in the fluorescence emission intensity at 457 nm was monitored. A blank titration of polylysine in the above buffer was performed and the signal contributed by the blank was subtracted from that of the sample. The difference in the emission intensity at 457 nm was plotted as a function of polylysine concentration. The dissociation constant for the hCA XII-polylysine complex was determined via analysis of the data as described by Qin and Srivastava [39]. The binding isotherm for the interaction of Qds^+ with hCA XII in the presence of DNSA was determined by titrating a fixed concentration of hCA XII and saturating concentrations of DNSA by increasing concentrations of Qds^+ in 10 mM Tris-

HCl buffer, pH 8.0, containing 10 % acetonitrile. The excitation and emission slits were kept at 10 mm each. The increase in the fluorescence intensity of Qds^+ (after subtracting the signal from free Qds^+) at 600 nm (λ_{ex} = 330 nm) is plotted as a function of Qds^+ concentration and the binding isotherm was analysed as mentioned above.

The dissociation constant of hCA XII-DNSA complex in the presence of saturating concentrations of polylysine was determined by titrating a fixed concentration of hCA XII and saturating concentrations of polylysine by increasing concentrations of DNSA in 25 mM HEPES buffer, pH 7.5, containing 10 % acetonitrile. The increase in the fluorescence emission intensity of hCA XII-DNSA complex at 457 nm (λ_{ex} = 330 nm) was monitored and was plotted as a function of total concentration of DNSA. The binding isotherm was determined via analysis of the data as described above.

Fluorescence Lifetime measurements—Fluorescence Lifetime measurements were performed on a Photon Technology International (PTI) Fluorescence-Lifetime Instrument. Light Emitting diodes (LEDs) with maximum power outputs at 280 nm and 340 nm were used as excitation sources for measuring the time resolved fluorescence decay. Whereas the 280 nm LED was utilized to excite the intrinsic fluorescence of the protein (primarily contributed by the tryptophan and tyrosine residues), the 340 nm LED was utilized to excite Qds^+. The emitted light was detected (at right angle of the excitation source) by means of a stroboscopic emission monochromator, configured at an appropriate wavelength. The time resolved fluorescence decay curves were analyzed to obtain the lifetimes of the fluorophores under different conditions by the aid of the PTI's software, Felix 32.

RESULTS

Except for a minor difference, the amino acid sequence of our hCA XII construct is essentially identical to that used for determining the crystal structure of the enzyme [40], and the purified form of the native protein was found to be homodimer of subunit molecular weight of 30 kD (see Experimental Procedures). In light of the X-ray crystallographic data, it is apparent that the enzyme harbors 8 tryptophan residues per subunit with varied degrees of exposures to the aqueous environment [40]. The intrinsic emission spectrum of the enzyme protein (λ_{ex} = 295 nm) yields a peak at 336 nm (Figure 1, Panel A). As described previously [34,41], Qds^+ are characterized by a very broad absorption spectrum ranging from far UV region to 650 nm with a small peak at 570 nm. When excited at 570 nm, the Qds^+ show a marked emission band at 610 nm [34]. Using these electronic signals, we probed the interaction between Qds^+ and hCA XII. As shown in Figure 1 (Panel A), the intrinsic fluorescence of hCA XII is quenched in the presence of near stoichiometric concentration of Qds^+. We confirmed that such a quenching was not an artifact of the inner filter effect since the absorption of the reaction mixture was less than 0.1. Evidently, the quenching of the enzyme's fluorescence by Qds^+ was due to hCA XII - Qds^+ interaction. This was not surprising since the electrostatic surface potential of hCA XII opposite to the active site pocket of the enzyme is predominantly negative [34,40]. Hence, the hCA XII - Qds^+ interaction was envisaged to be caused by the electrostatic forces. To ascertain this, we recorded the spectrum of hCA XII-Qds^+ in the presence of 250 mM NaCl (data not shown). It was observed that the presence of NaCl restored the fluorescence emission peak of hCA XII (which was quenched by Qds^+), supporting our hypothesis.

We utilized the signal for Qds^+ induced quenching of the enzyme fluorescence in assessing the binding affinity and stoichiometry of the hCA XII-Qds^+ complex. In this endeavor, we opted to titrate a fixed concentration of Qds^+ with increasing concentrations of the enzyme due to high absorption of Qds^+ at 295 nm as well as our inability to precisely determine its concentration,. As shown in Figure 1 (Panel B), the extent of quenching exhibited a nearly

linear dependence at lower concentration of hCA XII with overall profile being hyperbolic in nature. This was suggestive of a very tight binding of the enzyme to the Qds^+ surface. Under this situation, a significant fraction of free enzyme could be envisaged to be complexed with Qds^+ during the entire course of titration, and thus the total concentration of hCA XII could not be taken as the measure of its free concentration. This scenario led to the analysis of the titration data of Figure 1B by the quadratic equation which takes into account the bound versus free form of the titrant such as described by Qin and Srivastava [39]. The solid smooth line is the best fit of the data of Figure 1B [39] for the dissociation constant and stoichiometry of the hCA XII-Qds^+ complex as being equal to 0.32 μM and 4 molecules of hCA XII subunit bound to per molecule of Qds^+, respectively. Since hCA XII is a dimeric protein, the above stoichiometry can be taken as being equal to 2 dimeric enzyme per Qds^+ molecule.

Since the broad absorption band of Qds^+ overlaps with the emission peak (336 nm) of hCA XII, the observed fluorescence quenching of hCA XII in the presence of Qds^+ was envisaged to be possibly due to the fluorescence resonance energy transfer (FRET) from the tryptophan residues of hCA XII to Qds^+. To probe this possibility, we determined the intrinsic fluorescence lifetime of hCA XII in the absence and presence of Qds^+. In this experiment, a relatively high energy 280 nm LED was used as the excitation source, and the emission wavelength was set at 336 nm. Figure 2 shows the excited state life time traces of hCA XII in the absence and presence of Qds^+. Both these lifetime traces conformed to the biphasic rate equation yielding two life times (τ_1 and τ_2). Whereas the analysis of the experimental data (solid smooth lines) for free hCA XII yielded the short (τ_1) and long (τ_2) life times as being equal to 0.24 and 2.4 ns, respectively, those for the hCA XII - Qds^+ complex yielded the above parameters to be 0.22 and 2.3 ns, respectively. Note that these values are not too different, suggesting that Qds^+ mediated quenching is not due to perturbation of the excited state energy of the enzyme's intrinsic fluorophores. Evidently, there has been no FRET between the enzyme's tryptophan residues and the Qds^+. The facts that Qds^+ quench the intrinsic steady-state fluorescence of hCA XII but does not alter the lifetimes of the tryptophan moieties imply that the overall quenching process is a ground state phenomenon [41]. The latter could be manifested either due to the formation of the complex with lower extinction coefficient or due to an impaired transition of the complex from the ground state to the excited state [41–42].

To ascertain whether or not the electrostatic interaction between hCA XII and Qds^+ altered the structural-functional features of the enzyme, we performed a series of experiments involving fluorescence inhibitor dansylamide (DNSA) of the enzyme as well as polylysine as an analogous (positively charged) surface binding group of the enzyme. DNSA is known to bind at the hydrophobic active site pocket of CA isozymes and such interaction results in a blue shift, with a marked increase in the fluorescence emission intensity of the fluorophores [42–44]. Whereas free DNSA exhibits a fluorescence emission band at 536 nm (λ_{ex} = 330 nm), the enzyme bound form is characterized by a relatively intense emission band at 457 nm. We investigated the effect of binding of Qds^+ to hCA XII on the fluorescence properties of the enzyme bound DNSA. The idea was to ascertain whether or not the distally (i.e., opposite to the active site pocket of the enzyme) bound Qds^+ somehow altered the microenvironment of the enzyme bound DNSA (via long range conformational changes) and such feature modulated the spectral properties of the fluorophore. Toward this goal, we titrated a fixed concentration of hCA XII (300 nM) and saturating concentration of DNSA (2 μM) with increasing concentrations of Qds^+ and monitored the fluorescence emission profile of the hCA XII bound DNSA. As shown in Figure 3A, as the concentration of Qds^+ increases, the fluorescence intensity of the hCA XII-DNSA complex at 457 nm (λ_{ex} = 330 nm) decreases. This proceeds in concomitance with an increase in the fluorescence emission peak of Qds^+ at 600 nm. As a control, we performed the above experiment in the

absence of hCA XII (data not shown), and observed that neither did Qds^+ quench the DNSA fluorescence around 536 nm region nor did its fluorescence intensity increase at 600 nm. Hence, the Qds^+ mediated quenching of the DNSA fluorescence occurred only when the latter was bound to hCA XII, and the overall process was manifested via the direct (electrostatic) interaction between hCA XII and Qds^+.

The data of Figure 3A further revealed that the fluorescence spectral changes adhered to a common isosbestic point only at higher concentration of Qds^+; no common isosbestic point was observed at lower concentrations of Qds^+. These features are more pronounced in the difference spectra (i.e., the spectra of the mixture minus the individual species) of Figure 3B. We believe the lack of a common isosbestic point at lower concentration of Qds^+ is due to non-specific quenching of the 457 nm peak vis a vis the FRET between the enzyme bound DNSA and Qds^+ (see below). However, at this time, we cannot rule out the possibility of the changes in the binding affinity of DNSA for hCA XII (resulting in the re-equilibration of the free and enzyme bound DNSA) under the influence of Qds^+ (see below).

The spectral titration results of Figures 3A and 3B allowed us to determine the binding affinity of Qds^+ to hCA XII in the presence of DNSA, and compared the above parameter with that obtained for the direct binding of free Qds^+ with the enzyme (i.e., 0.32 μM; Panel B of Figure 1). Figure 3C shows the plot of ΔF_{600} (extracted from the difference spectra of Figure 3B) as a function of Qds^+. The analysis of the experimental data by fixing the stoichiometry of 0.25 (i.e. 1 Qds^+ bound to per enzyme subunit; Panel B of Figure 1) yielded the dissociation constant of Qds^+ for the DNSA bound hCA XII as being equal to 0.09 μM. The latter value is about 4 fold lower than that obtained for the binding of Qds^+ to the unliganded form of the enzyme. Evidently, the bound DNSA slightly increases the avidity of the enzyme for Qds^+.

The fact that the fluorescence emission peak of Qds^+ at 600 nm only increases when DNSA is bound to hCA XII (Figures 3A and B) and not with the free enzyme (data not shown) led to the suggestion that the excited state energy of the enzyme bound DNSA was transferred to Qds^+ (i.e., the FRET effect). This was plausible since fluorescence emission maximum of the enzyme bound DNSA (457 nm) coincided with the broad absorption/excitation band of Qds^+ in the above region [34]. To substantiate the occurrence of FRET between the above species, we compared the excited state fluorescence decay profiles of Qds^+ under different experimental conditions (Figure 4). By using 340 nm LED as the excitation source and setting the emission monochromator at 600 nm, we obtained the time decay of the excited state fluorescence intensity of 1 μM free Qds^+ (control; panel A), in the presence of 25 μM hCA XII (panel B), in the presence of 25 μM DNSA (panel C), and in the presence of 3 μM hCA XII and 15 μM DNSA. All the reaction traces conformed to the biphasic rate equation yielding two life times, τ_1 and τ_2. Whereas the lifetimes of free Qds^+ and those in the presence of free hCA XII and free DNSA were found to be nearly identical (τ_1 and τ_2 falling in the range of 1.3 and 7.3 ns, respectively), the second (longer) lifetime (τ_2) of Qds^+ in the presence of hCA XII-DNSA complex increased to 11.4 ns. Although we do not understand the origin of the shorter lifetime component (τ_1) of Qds^+, the increase in the magnitude of τ_2 only in the presence of the enzyme bound DNSA (but not with other components) substantiates the occurrence of FRET between the enzyme bound DNSA and Qds^+.

Effect of polylysine as the positively charged macromolecules

To assort the contribution of positive charges vis a vis the structural features of Qds^+ in eliciting the observed spectral changes (Figure 3A and 3B) and/or the binding profiles of Qds^+ with hCA XII in the absence (Figure 1) and presence (Figure 3C) of DNSA, we utilized polylysine as the positively charged macromolecules. Toward this objective, we first investigated the influence of binding of polylysine to hCA XII on the fluorescence emission

profile of the enzyme bound DNSA. Figure 5A shows the fluorescence emission spectra of hCA XII bound DNSA (λ_{ex} = 330 nm) as a function of increasing concentrations of intact polylysine molecule (rather than its monomeric amino acid residue; see Experimental Procedures). Note that as the concentration of polylysine increases, the fluorescence emission intensity of DNSA at 457 nm decreases. It should be pointed out that such a quenching of the enzyme bound DNSA fluorescence (at 457 nm) has also been evident in the presence of Qds^+ (Figures 3A and B) although the latter has been demonstrated to proceed in concomitance with FRET between the above fluorophores. Evidently, the positive charges of the interacting macromolecules (contributed either by Qds^+ or polylysine) serve as the primary determinant in modulating the fluorescence properties of the enzyme-bound DNSA. Figure 5B shows the decrease in the fluorescence intensity of the enzyme-bound DNSA at 457 nm as a function of polylysine concentration. The binding isotherm was analyzed by the same quadratic equation which takes into account the bound versus free form of the titrant [39], and was used for analyzing the Qds^+-hCA XII binding data (see Figure 1). The solid smooth line is the best fit of the data for the binding affinity of polylysine for hCA XII-DNSA conjugate as being equal to 6 μM. In contrast, the binding affinity of polylysine for hCA XII in the absence of bound DNSA was determined to be 3.3 μM (data not shown). Hence, the presence of DNSA did not significantly influence the binding affinity of hCA XII for polylysine.

The question arose whether Qds^+ and polylysine mediated quenching of the enzyme-bound DNSA fluorescence was partly due to the changes in the binding affinity of the enzyme-DNSA complex. This was important since the fluorescence emission maxima and the intensity of free (aqueous) DNSA are markedly different than those obtained in the presence of carbonic anhydrase isozymes [43–44]. It should be mentioned that we could not substantiate or refute the above possibility in the presence of Qds^+ due to its high absorption as well as its interference in the fluorescence signal of the enzyme-DNSA complex (data not shown). However, since the latter constraints were non-existent with polylysine, we could easily determine the influence of polylysine on the binding affinity of DNSA for hCA XII. Figure 6 shows the titration of a fixed concentration of hCA XII (0.2 μM) and saturating concentration of polylysine (25 μM) with increasing concentrations of DNSA (λ_{ex} = 330 nm, λ_{em} = 457 nm). The analysis of the experimental data yielded the binding affinity of DNSA for hCA XII (bound to polylysine) as being equal to 0.18 μM. It should be emphasized that this value is similar to the binding affinity of DNSA for free enzyme as being equal to 0.08 μM [34]. Hence, the enzyme bound polylysine had practically no effect on the dissociation constant of the enzyme-DNSA complex.

Influence of positively charged macromolecules on the catalytic activity of hCA XII

Given that both Qds^+ and polylysine macromolecules interacted with hCA XII with comparable binding affinities, and both these macromolecules influenced the fluorescence emission profile of the enzyme-bound DNSA, we proceeded to determine whether or not they elicited similar or different influence on the catalytic activity of the enzyme. Toward this goal, we measured the activity of hCA XII in the absence and presence of Qds^+, polylysine and DNSA via the pH drop method [36]. The data are summarized in Table 1. Note that the activity of the enzyme drastically decreases in the presence of 5 μM DNSA. This was expected since DNSA is known to coordinate with the active site resident Zn^{2+}, and by doing so precludes the hydration reaction of CO_2. On the other hand, there was a very small decrease (approximately 7 to 10 %) in the catalytic activity of the enzyme upon addition of saturating concentrations of either polylysine or Qds^+. Evidently, the catalytic machinery of hCA XII remained practically unaffected upon binding of the positively charged macromolecules. In contrast to these observations, we were surprised to note that whereas the inhibitory effect of DNSA was overcome (by about 70 %) by the presence of

Qds^+ but not by polylysine. Clearly, despite their marked similarity in binding to the surface of hCA XII, they elicited different influence in modulating the enzyme activity. As will be discussed in the next section, the above noted discriminatory effect of these cationic macromolecules is encoded in their "rigid" versus "flexible" structural features.

DISCUSSION

A cumulative account of the experimental data presented herein leads to the following conclusions. (1) Qds^+ and polylysine (representative of cationic macromolecules) electrostatically interact on the surface of the protein opposite to the active site pocket of human carbonic anhydrase XII (hCA XII). (2) Neither of these cationic macromolecules influences the catalytic activity of the "free" (i.e., unliganded) enzyme. (3) Qds^+ and polylysine exhibit different influence on the fluorescence emission properties of the enzyme bound DNSA (one of the potent inhibitors of the enzyme). (4) Whereas the inhibitory effect of DNSA is overcome upon binding of Qds^+ to the enzyme's surface, it remains unchanged upon binding of polylysine. Evidently, Qds^+ and polylysine differently modulate the microenvironment of the enzyme's active site pocket (via the long range interaction), and such feature is likely to be encoded in the "rigidity" versus "flexibility" of these cationic macromolecules.

In view of the negative electrostatic potentials of the enzyme surface opposite to the active site pocket of hCAXII [34,40], it is not surprising that cationic macromolecules (Qds^+ and polylysine) electrostatically interact with hCA XII. The latter feature is evident by the fact that the increase in the ionic strength of the buffer media abolishes the Qds^+ mediated quenching of the intrinsic fluorescence of the enzyme. In addition, since neither the binding of DNSA nor the enzyme activity is altered particularly in the presence of polylysine (see Results), we are tempted to speculate that these cationic macromolecules interact on the enzyme surface opposite to the active site pocket of the enzyme.

Due to "colorless" nature of polylysine, it has been possible to decipher its influence on the fluorescence spectral profiles of the enzyme-bound DNSA and determine the dissociation constant of the enzyme-DNSA complex. We [43,44] and others [45–48] have provided evidence that the fluorescence spectral changes of free DNSA upon binding with carbonic anhydrases are contributed both by the hydrophobicity of the enzyme's active site pocket as well as the interaction of the deprotonated amide nitrogen of the sulfonamide group of the fluorophore to the enzyme resident Zn^{2+} cofactor. Hence, the apparent quenching of the fluorescence intensity (λ_{ex} = 330 nm, λ_{em}= 457 nm) of the enzyme-bound DNSA upon titration with polylysine (Figure 5A) can occur due a variety of reasons: (1) decrease in the binding affinity of DNSA for hCA XII in the presence of polylysine. Since the fluorescence intensity of free DNSA is significantly lower than that of its enzyme-bound form [45–49], its dissociation from the enzyme site (induced by polylysine) would result in the decrease in the fluorescence emission intensity. (2) Distortion of interaction between the enzyme resident Zn^{2+} cofactor and the amide nitrogen of DNSA. (3) Increase in polarity of the enzyme's active site pocket. However, irrespective of the mechanistic origin for the polylysine induced quenching of the DNSA fluorescence, the overall process must be coordinated via the long range (possibly subtle) changes in the protein conformation.

Of different plausible reasons for the polylysine-mediated quenching of the enzyme-bound DNSA fluorescence, the decrease in the binding affinity of the enzyme-DNSA complex (reason# 1) is unlikely. This is because the K_d value for hCA XII-DNSA complex (0.08 μM) remains practically unchanged in the presence of saturating concentration of polylysine (K_d = 0.18 μM). Furthermore, the effect of polylysine in distorting the interaction between the enzyme bound Zn^{2+} cofactor and the sulfonamide nitrogen of the fluorophore (reason #2) is

also unlikely since the activity of the DNSA inhibited enzyme is not regained in the presence of polylysine (Note that this is in contrast to the restoration of the DNSA inhibited activity of the enzyme in the presence of Qds^+; Table 1). Hence, the polylysine mediated quenching of the enzyme bound DNSA fluorescence is, at the best, due to increase in the polarity (reason #3) of the enzyme's active site pocket. The latter can easily happen due to increase in the extent of hydration of the active site pocket (in the vicinity of bound DNSA) via polylysine induced subtle changes in the enzyme conformation.

Unlike polylysine, Qds^+ induces marked changes in the fluorescence profile of the enzyme bound DNSA. This is also because Qds^+ itself is a fluorescent macromolecule and it accepts excited state energy from the enzyme bound DNSA (the FRET effect). Hence, the magnitude of quenching of the enzyme bound DNSA fluorescence (around 450 nm region) is likely to be caused by a combination of the Qds^+ mediated changes in the active site environment of the enzyme (akin to that noted with polylysine) and the FRET between the two fluorophores. This is further supported by the fact that Qds^+ dependent fluorescence spectral changes of the enzyme bound DNSA (Figure 3) is devoid of clean isosbestic point around 540 nm region. Since we could not determine the binding affinity of DNSA for hCA XII in the presence of Qds^+ (due to its interference in the observed fluorescence signal), the observed spectral changes of Figure 3 can also be contributed by a partial dissociation of DNSA from the enzyme site. However, in marked contrast to polylysine, the presence of Qds^+ overcomes the DNSA dependent inhibition of the enzyme (Table 1). Whether it is caused by the distortion and/or displacement of DNSA from the enzyme site, it appears likely that the binding of Qds^+ to hCA XII induces more pronounced changes at the active site pocket of the enzyme than its cationic macromolecular counterpart - polylysine.

The question arises why similarly charged cationic macromolecules (Qds^+ and polylysine) differently influence the microenvironment of the enzyme's active site? In attempting to answer this question, we note that whereas Qds^+ is a representative of a "rigid" charge carrier, polylysine is a "flexible" cationic macromolecule. Hence, the binding of hCA XII on the Qds^+ surface can result in the bending/flexing of the enzyme structure, resulting in the long range influence on the structural feature of the enzyme's active site pocket. On the other hand, due to flexible nature of polylysine, its binding with the enzyme can result in readjusting its structure. In view of these arguments, we propose that the Qds^+ mediated changes (via long range interaction) at the active site pocket of the enzyme abolishes the interaction of the Zn^{2+} cofactor with the sulfonamide nitrogen of DNSA. This occurs presumably due to creation of new binding site of DNSA that is somewhat removed from its original binding site at the active site pocket of the enzyme. As a consequence, Zn^{2+}-OH^- is generated at the active site, and it serves as the Lewis acid-base pair in facilitating the hydration of CO_2 (see the cartoon of Figure 7). Being small molecules, CO_2 and H_2O can easily diffuse in the vicinity of the Zn^{2+} cofactor, promoting the carbonic anhydrase catalyzed reaction of $CO_2 + H_2O \rightleftharpoons HCO_3^- + H^+$. This is in marked contrast to the miniscule influence of polylysine on the configuration of DNSA within the enzyme's active site pocket, and thus it does not facilitate the enzyme catalysis.

The effects of differently functionalized nanoparticles (as well as their shapes and sizes) on the structural-functional features of enzymes has been reviewed by Wu et al ([50]. Depending on the nature of the enzymes and complementarily charged nanoparticles, the electrostatic interactions can range from being silent to inhibition and inactivation of enzymes. For example, Rotello and his collaborators [51] have elegantly demonstrated that the electrostatic interaction between anionic gold nanoparticles and chymotrypsin results in the instantaneous inhibition of the enzyme activity followed by its inactivation on a longer time scale. The latter effect has been found to proceed in concomitance with changes in the secondary structural feature of the enzyme. Among carbonic anhydrase isozymes, the

interaction between negatively charged silica nanoparticles and hCA II has been reported by Karlsson and Carlsson [52]. These, in conjunction with other literature data [27–32], strengthens our deduction that the changes in the functional features of hCA XII are manifested via the structural changes in the protein, and the latter occurs via the long range interaction, akin to the allosteric modulation of the enzymatic function [53]. Whether or not the discriminatory influence of the “rigid” versus “flexible” macromolecules on hCA XII is unique is currently being investigated in our lab.

Acknowledgments

This research was supported by the National Institutes of Health (NIH) grants CA113746, CA132034 and National Science Foundation (NSF) grant DMR-0705767 to D.K.S. Sumathra Manokaran was supported by the National science foundation - Experimental Program to Stimulate Competitive Research Award EPS-0814442. Wei Chen would like to thank the support by the Startup funds from UTA, the NSF and DHS joint program (2008-DN-077-ARI016-03), and the U.S. Army Medical Research Acquisition Activity (USAMRAA) under Contract No.W81XWH-05-C-0101 and BC095348.

ABBREVIATIONS

CA	Carbonic anhydrase
hCA XII	human carbonic anhydrase XII
DNSA	dansylamide
CdTe	Cadmium telluride
Qds	CdTe quantum dots
Qds$^+$	positively charged quantum dots
EDTA	Ethylene diamine tetra acetic acid
PMSF	phenylmethylsulfonyl fluoride
IPTG	Isopropyl-beta-D-thiogalactopyranoside

References

1. Bruchez M, Moronne M, Gin P, Weiss S, Alivisatos AP. Semiconductor nanocrystals as fluorescent biological labels. Science. 1998; 281:2013–2016. [PubMed: 9748157]
2. Chan WCW, Nie S. Quantum dot bioconjugates for ultrasensitive nonisotopic detection. Science. 1998; 281:2016–2018. [PubMed: 9748158]
3. Michalet X, Pinaud FF, Bentolila LA, Tsay JM, Doose S, Li JJ, Sundaresan G, Wu AM, Gambhir SS, Weiss S. Quantum dots for live cells, in vivo imaging, and diagnostics. Science. 2005; 307:538–544. [PubMed: 15681376]
4. Wu X, Liu H, Liu J, Haley KN, Treadway JA, Larson JP, Ge N, Peale F, Bruchez MP. Immunofluorescent labeling of cancer marker Her2 and other cellular targets with semiconductor quantum dots. Nat Biotech. 2003; 21:41–46.
5. Alivisatos AP. Semiconductor clusters, nanocrystals, and quantum dots. Science. 1996; 271:933–937.
6. Murray CB, Norris DJ, Bawendi MG. Synthesis and characterization of nearly monodisperse CdE (E = sulfur, selenium, tellurium) semiconductor nanocrystallites. J Am Chem Soc. 1993; 115:8706–8715.
7. Dabbousi BO, Rodriguez-Viejo J, Mikulec FV, Heine JR, Mattoussi H, Ober R, Jensen KF, Bawendi MG. (CdSe)ZnS Core-shell quantum dots: Synthesis and characterization of a size series of highly luminescent nanocrystallites. J Phys Chem B. 1997; 101:9463–9475.
8. Gaponenko, SV. Optical properties of semiconductor nanocrystals. 1. Cambridge University Press; 1998.

9. Resch-Genger U, Grabolle M, Cavaliere-Jaricot S, Nitschke R, Nann T. Quantum dots versus organic dyes as fluorescent labels. Nat Methods. 2008; 5:763–775. [PubMed: 18756197]
10. Chen W. Nanoparticle fluorescence based technology for biological applications. J Nanosci Nanotechnol. 2008; 8:1019–1051. [PubMed: 18468106]
11. Bharali DJ, Klejbor I, Stachowiak EK, Dutta P, Roy I, Kaur N, Bergey EJ, Prasad PN, Stachowiak MK. Organically modified silica nanoparticles: A nonviral vector for in vivo gene delivery and expression in the brain. Proc Natl Acad Sci U S A. 2005; 102:11539–11544. [PubMed: 16051701]
12. Nel A, Xia T, Madler L, Li N. Toxic potential of materials at the nanolevel. Science. 2006; 311:622–627. [PubMed: 16456071]
13. Service RF. Science policy: Priorities needed for nano-risk research and development. Science. 2006; 314:45. [PubMed: 17023629]
14. Barnard AS. Nanohazards: Knowledge is our first defence. Nat Mater. 2006; 5:245–248. [PubMed: 16582921]
15. Inoue KI, Takano H, Yanagisawa R, Hirano S, Sakurai M, Shimada A, Yoshikawa T. Effects of airway exposure to nanoparticles on lung inflammation induced by bacterial endotoxin in mice. EnViron Health Perspect. 2006; 114:1325–1330. [PubMed: 16966083]
16. Sayes CM, Wahi R, Kurian PA, Liu Y, West JL, Ausman KD, Warheit DB, Colvin VL. Correlating nanoscale titania structure with toxicity: A cytotoxicity and inflammatory response study with human dermal fibroblasts and human lung epithelial cells. Toxicol Sci. 2006; 92:174–185. [PubMed: 16613837]
17. Howarth M, Takao K, Hayashi Y, Ting AY. Targeting quantum dots to surface proteins in living cells with biotin ligase. Proc Natl Acad Sci. 2005; 102:7583–7588. [PubMed: 15897449]
18. Xiao Y, Barker PE. Semiconductor nanocrystal probes for human metaphase chromosomes. Nucl Acids Res. 2004; 32:e28. [PubMed: 14960711]
19. Crut A, Geron-Landre B, Bonnet I, Bonneau S, Desbiolles P, Escude C. Detection of single DNA molecules by multicolor quantum-dot end-labeling. Nucl Acids Res. 2005; 33:e98. [PubMed: 15967805]
20. Lynch I, Dawson KA, Linse S. Detecting cryptic epitopes created by nanoparticles. Science STKE. 2006; 327:pe14.
21. Shao L, Dong C, Sang F, Qian H, Ren J. Studies on interaction of CdTe quantum dots with bovine serum albumin using fluorescence correlation spectroscopy. J Fluoresc. 2009; 19:151–157. [PubMed: 18607697]
22. You CC, Arvizo RR, Rotello VM. Regulation of alpha-chymotrypsin activity on the surface of substrate-functionalized gold nanoparticles. Chem Commun. 2006; 27:2905–2907.
23. Irle S, Zheng G, Elstner M, Morokuma K. Formation of fullerene molecules from carbon Nanotubes: A quantum chemical molecular dynamics study. Nano Lett. 2003; 3:465–470.
24. Erlanger BF, Chen B, Zhu M, Brus L. Binding of an anti-fullerene IgG monoclonal antibody to single wall carbon nanotubes. Nano Lett. 2001; 1:465–467.
25. Chen RJ, Zhang Y, Wang D, Dai H. Noncovalent sidewall functionalization of single-walled carbon nanotubes for protein immobilization. J Am Chem Soc. 2001; 123:3838–3839. [PubMed: 11457124]
26. Hong R, Emrick T, Rotello VM. Monolayer-controlled substrate selectivity using noncovalent enzyme-nanoparticle conjugates. J Am Chem Soc. 2004; 126:13572–13573. [PubMed: 15493887]
27. Shen X, Liou X, Ye L, Liang H, Wang Z. Spectroscopic studies on the interaction between human hemoglobin and CdS quantum dots. J Colloid Interface Sci. 2007; 311:400–406. [PubMed: 17433354]
28. Lundqvist M, Sethson I, Jonsson B. High-resolution 2D 1H-15N NMR characterization of persistent structural alterations of proteins induced by interactions with silica nanoparticles. Langmuir. 2005; 21:5974–5979. [PubMed: 15952849]
29. Norde W, Giacomelli CE. BSA structural changes during homomolecular exchange between the adsorbed and the dissolved states. J Biotechnol. 2000; 79:259–268. [PubMed: 10867186]
30. Wu X, Narsimhan G. Effect of surface concentration on secondary and tertiary conformational changes of lysozyme adsorbed on silica nanoparticles. Biochim Biophys Acta. 2008; 1784:1694–1701. [PubMed: 18638578]

31. Vertegel AA, Siegel RW, Dordick JS. Silica nanoparticle size influences the structure and enzymatic activity of adsorbed lysozyme. Langmuir. 2004; 20:6800–6807. [PubMed: 15274588]
32. Shang W, Nuffer JH, Dordick JS, Siegel RW. Unfolding of ribonuclease A on silica nanoparticle surfaces. Nano Lett. 2007; 7:1991–1995. [PubMed: 17559285]
33. Wang L, Chen H, Wang L, Li L, Xu F, Liu J, Zhu C. Preparation and application of a novel composite nanoparticle as a protein fluorescence probe. Anal Lett. 2004; 37:213.
34. Manokaran S, Berg A, Zhang X, Chen W, Srivastava DK. Modulation of ligand binding affinity of tumorigenic carbonic anhydrase XII upon interaction with cationic CdTe quantum dots. J Biomed Nanotech. 2008; 4:491–498.
35. Sambrook, J.; Fritsch, E.; Maniatis, T. Molecular Cloning: A laboratory Manual. Cold Spring Harbor Laboratory Press; Plainview, NY: 2000.
36. Wilbur KM, Anderson NG. Electrometric and colorimetric determination of carbonic anhydrase. J Biol Chem. 1948; 176:147–154. [PubMed: 18886152]
37. Bradford MM. A rapid and sensitive method for the quantitation of microgram quantities of protein utilizing the principle of protein-dye binding. Anal Biochem. 1976; 72:248–254. [PubMed: 942051]
38. Weber K, Osborn M. The reliability of molecular weight determinations by dodecyl sulfate polyacrylamide gel electrophoresis. J Biol Chem. 1969; 244:4406–4412. [PubMed: 5806584]
39. Qin L, Srivastava DK. Energetics of two-step binding of a chromophoric reaction product, trans-3-indoleacryloyl-CoA, to medium-chain acyl-coenzyme-A dehydrogenase. Biochemistry. 1998; 37:3499–3508. [PubMed: 9521671]
40. Whittington DA, Waheed A, Ulmasov B, Shah GN, Grubb JH, Sly WS, Christianson DW. Crystal structure of the dimeric extracellular domain of human carbonic anhydrase XII, a bitopic membrane protein overexpressed in certain cancer tumor cells. Proc Natl Acad Sci U S A. 2001; 98:9545–9550. [PubMed: 11493685]
41. Joly AG, Chen W, McCready DE, Malm J, Bovin J. Upconversion luminescence of CdTe nanoparticles. Phys Rev B. 2005; 71:165304–165313.
42. Lakowicz, JR. Principles of fluorescence spectroscopy. 2. Kluwer Academic/Plenum Publishers; New York: 1999.
43. Banerjee AL, Tobwala S, Ganguly B, Mallik S, Srivastava DK. Molecular basis for the origin of differential spectral and binding profiles of dansylamide with human carbonic anhydrase I and II. Biochemistry. 2005; 44:3673–3682. [PubMed: 15751944]
44. Banerjee J, Haldar MK, Manokaran S, Mallik S, Srivastava DK. New fluorescent probes for carbonic anhydrases. Chem Commun. 2007; 38:2723–2725.
45. Chen RF, Kernohan JC. Combination of bovine carbonic anhydrase with a fluorescent sulfonamide. J Biol Chem. 1967; 242:5813–5823. [PubMed: 4990698]
46. Day YSN, Baird CL, Rich RL, Myszka DG. Direct comparison of binding equilibrium, thermodynamic, and rate constants determined by surface- and solution-based biophysical methods. Protein Sci. 2002; 11:1017–1025. [PubMed: 11967359]
47. Fierke CA, Calderone TL, Krebs JF. Functional consequences of engineering the hydrophobic pocket of carbonic anhydrase II. Biochemistry. 1991; 30:11054–11063. [PubMed: 1657158]
48. Nair SK, Krebs JF, Christianson DW, Fierke CA. Structural basis of inhibitor affinity to variants of human carbonic anhydrase II. Biochemistry. 1995; 34:3981–3989. [PubMed: 7696263]
49. Banerjee AL, Swanson M, Roy BC, Jia X, Haldar MK, Mallik S, Srivastava DK. Protein surface-assisted enhancement in the binding affinity of an inhibitor for recombinant human carbonic anhydrase-II. J Am Chem Soc. 2004; 126:10875–10883. [PubMed: 15339172]
50. Wu Z, Zhang B, Yan B. Regulation of enzyme activity through interactions with nanoparticles. Int J Mol Sci. 2009; 10:4198–4209. [PubMed: 20057940]
51. Fischer NO, McIntosh CM, Simard JM, Rotello VM. Inhibition of chymotrypsin through surface binding using nanoparticle-based receptors. Proc Natl Acad Sci U S A. 2002; 99:5018–5023. [PubMed: 11929986]
52. Karlsson M, Carlsson U. Protein adsorption orientation in the light of fluorescent probes: Mapping of the interaction between site-directly labeled human carbonic anhydrase II and silica nanoparticles. Biophys J. 2005; 88:3536–3544. [PubMed: 15731384]

53. Monod J, Wyman J, Changeux JP. On the nature of allosteric ransitions: a plausible model. J Mol Biol. 1965; 12:88–118. [PubMed: 14343300]

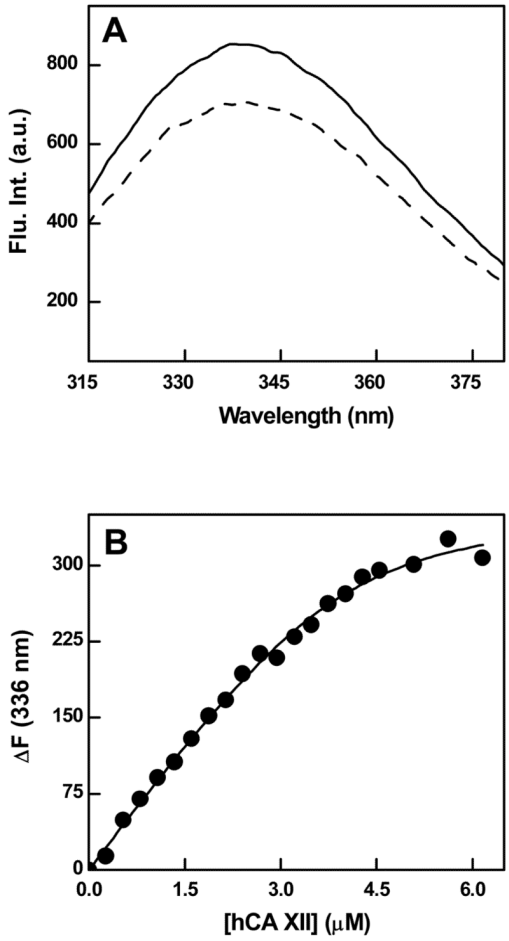

Figure 1.

Quenching of the intrinsic fluorescence of hCA XII upon binding of Qds^+. Panel A shows the fluorescence emission spectra of hCA XII (0.2 μM; λ_{ex} = 295 nm) in the absence (solid line) and presence (broken line) of 0.2 μM Qds^+ in 10 mM Tris-HCl buffer pH 8.0. Panel B shows the binding isotherm for the interaction of hCA XII with Qds^+ under the above experimental condition. [Qds^+] = 0.96 μM. The solid smooth line is the best fit of the data for a dissociation constant of 0.32 ± 0.16 μM and the stoichiometry of 4 hCA XII subunit bound per molecule of Qds^+.

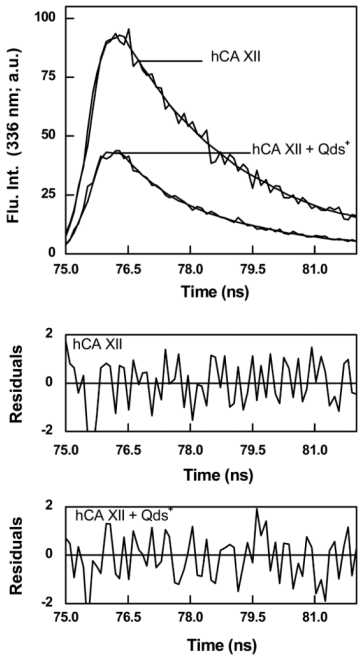

Figure 2.

Excited state fluorescence decay profiles of hCA XII in the absence and presence of Qds^+. [hCA XII] = 1 μM; [Qds^+] = 11 μM; λ_{ex} = 280 nm; λ_{em} = 336 nm. Other experimental conditions are same as in Figure 1. The solid smooth lines are the best fit of the data for the double exponential rate equation with τ_1 = 0.24 ± 0.01 ns and τ_2 =2.4 ± 0.01 ns in the absence of Qds^+ , and τ_1 = 0.22 ± 0.01 ns and τ_2 =2.3 ± 0.03 ns in the presence of Qds^+. The bottom panels show the residuals of the fitted data.

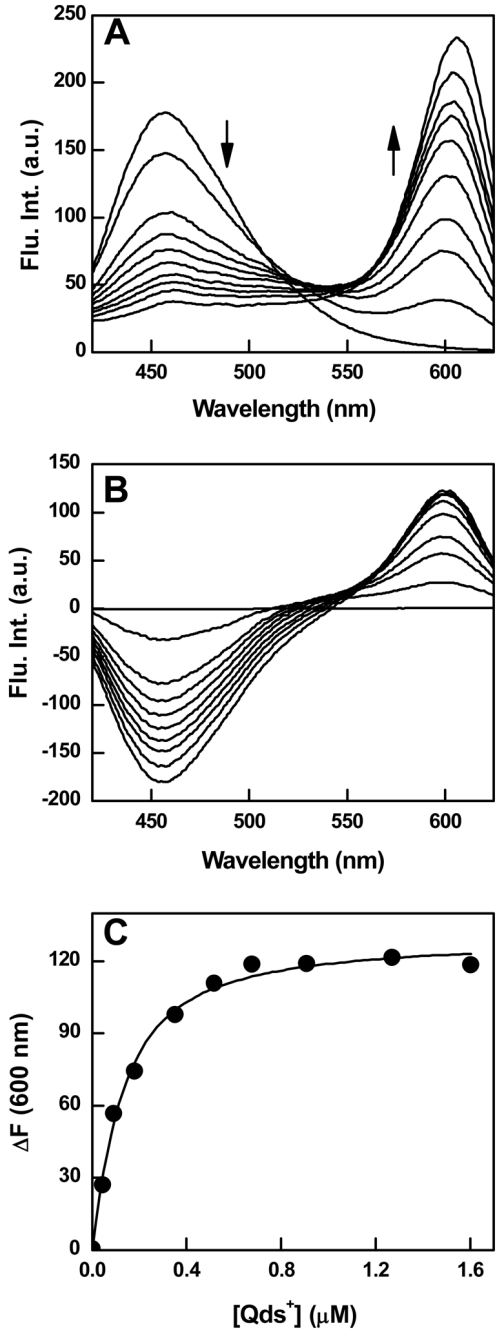

Figure 3.

Fluorescence spectral changes and binding isotherm for the interaction of Qds^+ with hCA XII-DNSA complex. Panel A shows the spectra of hCA XII-DNSA complex in the presence of increasing concentrations of Qds^+ in 10 mM Tris-HCl buffer, pH 8.0 containing 10 % acetonitrile. [hCA XII] = 0.3 μM, [DNSA] = 2 μM, λ_{ex} = 330 nm. The decrease and increase in the fluorescence emission intensity at 457 and 600 nm, respectively, are shown by the arrows. Panel B shows the difference spectra, which were derived from the raw spectral data of Panel A minus the sum of the spectra of the individual components. Panel C shows the plot of ΔF_{600} (from panel B) as a function of Qds^+ concentration. The solid smooth line is the best fit of the data (by fixing the stoichiometry of 0.25, the value reciprocal of the

experimentally determined stoichiometry of hCAXII-Qds^{+} complex; Figure 1) for the dissociation constant of hCA XII (DNSA)-Qds^{+} complex as being equal to 0.09 ± 0.01μM.

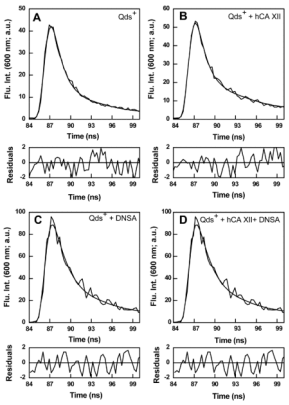

Figure 4.

Fluorescence lifetimes of Qds^+ under various conditions. Excited state fluorescence decay profiles of free Qds^+ (1 μM) (Panel A), Qds^+ (1 μM) in the presence of 25 μM hCA XII (Panel B), Qds^+ (1 μM) in the presence of 25 μM DNSA (Panel C), Qds^+ (1 μM) in the presence of 3 μM hCA XII and 15 μM DNSA (Panel D). The excitation and emission wavelengths were 340 nm and 600 nm, respectively. Other experimental conditions were same as in Figure 3. The solid smooth lines are the best fit of the data according to the double exponential rate equation for the data of different panels. Panel A: $\tau_1 = 1.3 \pm 0.01$ ns; $\tau_2 = 7.3 \pm 0.02$ ns; Panel B: $\tau_1 = 1.3 \pm 0.01$ ns ; $\tau_2 = 7.3 \pm 0.01$ ns. Panel C: $\tau_1 = 1.4 \pm 0.02$ ns; $\tau_2 = 7.4 \pm 0.01$ ns. Panel D: $\tau_1 = 1.4 \pm 0.02$ ns; $\tau_2 = 11.4 \pm 0.02$ ns. The bottom panels show the residuals of the fitted data.

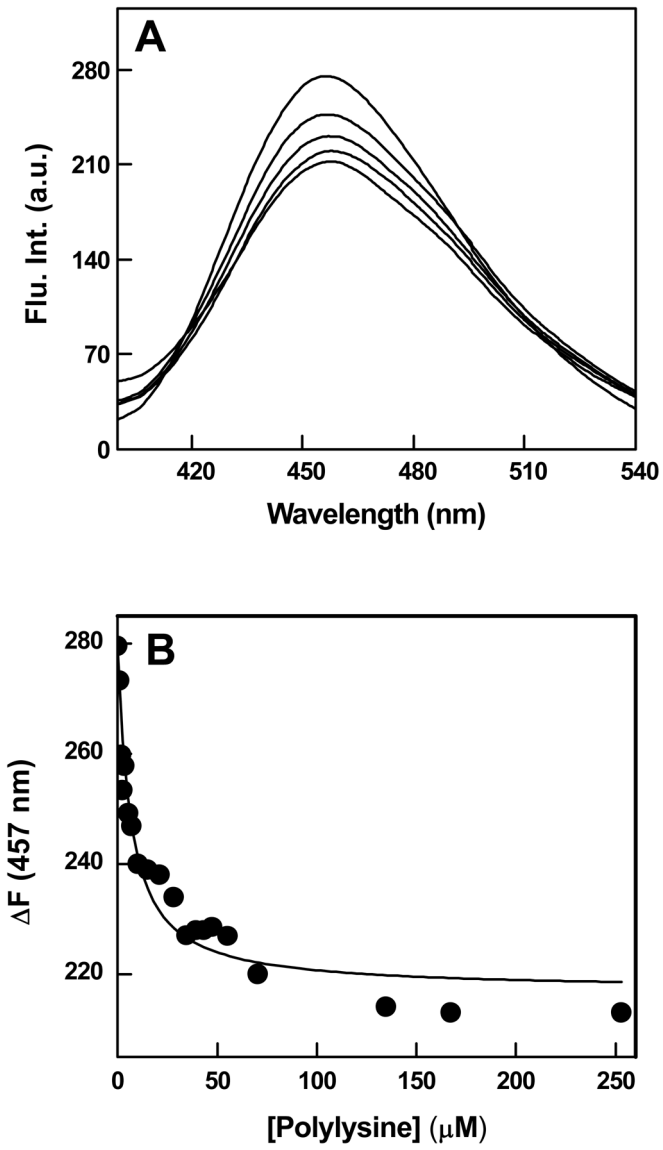

Figure 5.

Fluorescence spectral changes upon binding of polylysine with hCA XII-DNSA complex. Panel A shows the fluorescence emission spectra of hCA XII-DNSA complex in the presence of increasing concentrations of polylysine. The experiments were performed in 25 mM HEPES buffer, pH 7.5 containing 10% Acetonitrile. [hCA XII] = 1 μM, [DNSA] = 5 μM, polylysine = [1-253 μM], λ_{ex} = 330 nm. Panel B shows the binding isotherm for the interaction of polylysine with hCA XII- DNSA complex. The decrease in the fluorescence emission intensity of hCA XII-DNSA at 457 nm (derived from the data of Panel A) was plotted as a function of polylysine concentration. The solid smooth line is the best fit of the data for the dissociation constant of hCA XII(DNSA)-polylysine complex as being equal to 6 ± 0.9 μM.

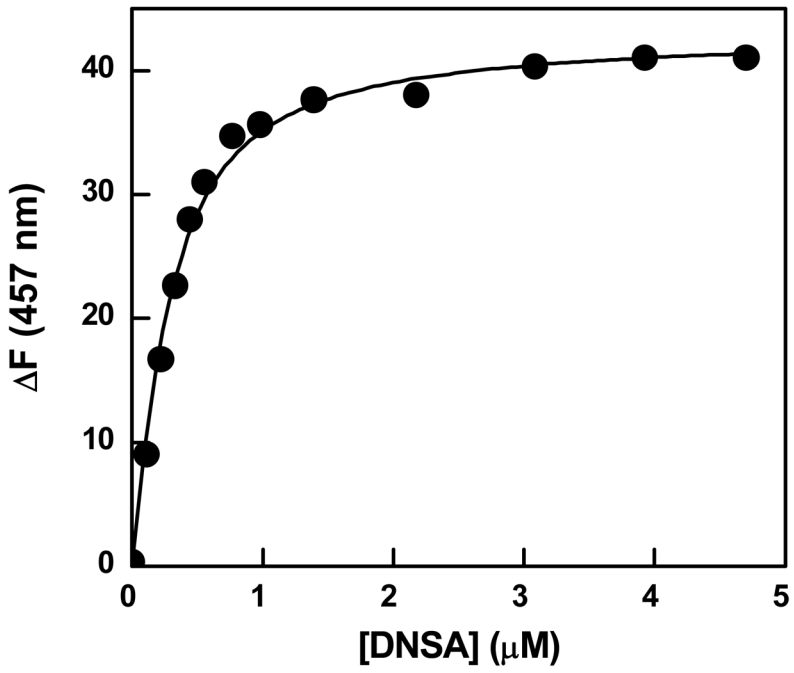

Figure 6.

Effect of polylysine on the binding affinity of DNSA with hCA XII. A fixed concentration of hCA XII (0.2 μM) with saturating concentrations of polylysine (25 μM) was titrated with increasing concentrations of DNSA, and the increase in the fluorescence emission intensity of hCA XII-DNSA complex at 457 nm (λ_{ex} = 330 nm) was monitored. The experimental condition was same as in Figure 5. The solid smooth line is the best fit of the data for the K_d value of 0.18 ± 0.01 μM.

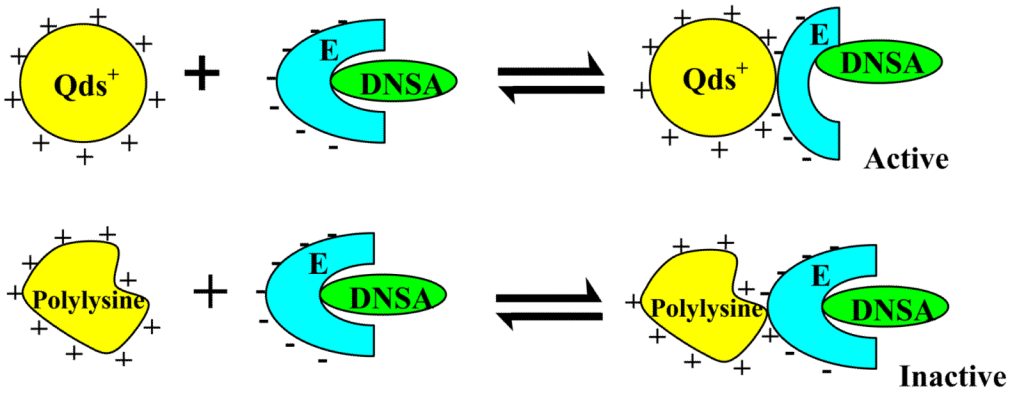

Figure 7.

Diagrammatic representations for the differential influence of Qds^+ and polylysine on the microenvironment of the active site pocket of hCA XII. It is surmised that unlike polylysine, the binding of Qds^+ to hCA XII alters the microenvironment of the enzyme's active site pocket, resulting in reorientation of the Zn^{2+}-ligated DNSA and thus overcoming the inhibitory effect of DNSA. Since such changes are not manifested upon binding of polylysine to hCA XII (DNSA) complex and thus the enzyme remains inhibited.

Table 1

Catalytic activity of hCA XII in the presence of different ligands[1]

Experimental condition[2]	% Activity
Free hCA XII	100
hCA XII –DNSA	9
hCA XII-Qds^{+}	92
hCA XII-DNSA -Qds^{+}	72
hCA XII-Polylysine	91
hCA XII-DNSA-Polylysine	2

[1] All experiments have been performed under identical condition, and the enzyme activity is represented as the percent of the control activity in the absence of any added Ligand.

[2] [DNSA]= 5 μM, [Polylysine] = 25 μM, [Qds^{+}] = 10 μM.